FABAD J. Pharm. Sci., 51, 1, 1-22, 2026
Doi: 10.55262/fabadeczacilik.1792162
RESEARCH ARTICLE

Investigation of Benzothiazole-Schiff Bases for Antimicrobial Activities Through ADMET, Molecular Docking, and DFT Analysis

Augustine Onuche SULE*, Olatunde ABIMBOLA MODUPE**, Banjo SEMIRE***°

Investigation of Benzothiazole-Schiff Bases for Antimicrobial Activities Through ADMET, Molecular Docking, and DFT Analysis

SUMMARY

Antimicrobial resistance is a critical global health issue, driving the urgent need for novel antimicrobial agents. This study employs an integrated computational framework combining Density Functional Theory (DFT), molecular docking, and ADMET profiling to evaluate the antibacterial potential of four benzothiazole-Schiff base hybrids (S08, S13, S15, S19). DFT calculations revealed that the hybrids possess lower HOMO-LUMO energy gaps (4.05-4.11 eV) and higher electrophilicity indices (2.669-3.156 eV) than ciprofloxacin, indicating enhanced chemical reactivity that correlates with their potent experimental Minimum Inhibitory Concentrations (MICs: 3.91-15.6 µg/mL). Molecular docking demonstrated strong binding affinities to bacterial DNA gyrase targets (Staphylococcus aureus Gyrase B and Escherichia coli Gyrase B), with key interactions identified at the atomic level. Crucially, ADMET profiling designated S19 as the lead candidate, exhibiting a favorable drug-likeness profile, high gastrointestinal absorption, and a superior safety profile, being non-mutagenic and devoid of hERG cardiotoxicity risks. This comprehensive in silico investigation provides profound insights into the structure-activity-toxicity relationships of these hybrids and firmly nominates S19 as a promising lead compound for subsequent synthesis and experimental development as a novel antimicrobial agent.

Keywords: *Schiff bases, MIC, DFT, molecular docking, and ADMET.*

ADMET, Moleküler Yerleştirme ve DFT Analizi ile Benzotiyazol-Schiff Bazlarının Antimikrobiyal Aktivitelerinin İncelenmesi

ÖZ

Antimikrobiyal direnç, yeni antimikrobiyal ajanlara olan acil ihtiyacı artıran kritik bir küresel sağlık sorunudur. Bu çalışma, dört benzotiyazol-Schiff baz hibritinin (S08, S13, S15, S19) antibakteriyel potansiyelini değerlendirmek için Yoğunluk Fonksiyonel Teorisi (DFT), moleküler yerleştirme ve ADMET profillemesini birleştiren entegre bir hesaplamalı çerçeve kullanmaktadır. DFT hesaplamaları, hibritlerin siprofloksasinden daha düşük HOMO-LUMO enerji aralıklarına (4,05 - 4,11 eV) ve daha yüksek elektrofilisite indekslerine (2,669 - 3,156 eV) sahip olduğunu ortaya koymuştur; bu da, güçlü deneysel Minimum İnhibitör Konsantrasyonları (MİK: 3,91 - 15,6 µg/mL) ile korelasyon gösteren artan kimyasal reaktiviteye işaret etmektedir. Moleküler yerleştirme, bakteriyel DNA giraz hedeflerine (Staphylococcus aureus Giraz B ve Escherichia coli Giraz B) karşı güçlü bağlanma afiniteleri gösterdi ve atomik düzeyde anahtar etkileşimler tanımlandı. En önemlisi, ADMET profillemesi, uygun bir ilaç-benzeri profil, yüksek gastrointestinal emilim ve üstün bir güvenlik profili sergileyen (mutajenik olmaması ve hERG kardiyotoksisite risklerinden arınmış olması nedeniyle) S19'u öncü aday olarak belirledi. Bu kapsamlı in siliko araştırma, bu hibritlerin yapı-aktivite-toksisite ilişkilerine dair derin içgörüler sağlamakta ve S19'u, yeni bir antimikrobiyal ajan olarak sonraki sentez ve deneysel geliştirme için umut verici bir öncü bileşik olarak kesin bir şekilde önermektedir.

Anahtar Kelimeler: *Schiff bazları, MİK, DFT, moleküler yerleştirme, ADMET.*

Recieved: 27.09.2025
Revised: 31.10.2025
Accepted: 4.11.2025

* ORCID: 0009-0006-3953-209X, Department of Chemistry, Federal University, Lokoja, Nigeria
** ORCID: 0000-0002-6253-8645, Department of Chemistry, University of Ibadan, Ibadan, Oyo State, Nigeria
*** ORCID: 0000-0002-4173-9165, Computational Chemistry Research Laboratory, Department of Pure and Applied Chemistry, Ladoke Akintola University of Technology, Ogbomoso, Nigeria

° Corresponding Author; Banjo SEMIRE
E-mail: bsemire@latech.edu.ng

INTRODUCTION

Current resistance to antibiotics hinders the efficacy of therapeutics, leading to further spread of infectious diseases. This underscores the pressing necessity for the development of an innovative class of antimicrobial compounds (Singh et al., 2017). Modern pharmacological design is heavily dependent on heterocyclic compounds, which can mimic biomolecules and engage in selective interactions with biological receptor complexes (Pibiri, 2024). These features provide a potent framework for adjusting physicochemical characteristics such as polarity and solubility, pharmacokinetic (ADME) profile, and toxicity of the drug candidate (Hahn, 2024).

By combining aldehydes or ketones with amines in a condensation reaction, an imine (-C=N-) bond is formed, replacing the carbonyl (–C=O) group and creating a major subclass of Schiff bases (Abdel Aziz, Ramadan, Sidqi, & Sayed, 2023; Babaei, Rezvan, Gilani, & Mansour, 2024). The presence of an imine linkage in the Schiff base molecules is essential for exhibiting this compound's wide spectrum of biological applications, like analgesic (Yassen & AL-Azzawi, 2023), anticancer (Alasadi, Jumaa, & Mukhlif, 2023; Aroua et al., 2023), antimicrobial (Alfonso-Herrera et al., 2022; Awolope, Ejidike, & Clayton, 2022), antitumor (Rezaei et al., 2023), antioxidant (Abd El-Hamid, Sadeek, Mohammed, Ahmed, & El-Gedamy, 2023; Aytac, Gundogdu, Bingol, & Gulcin, 2023), antiviral (Pore et al., 2023) and anti-inflammatory activity (Krishna, Dhanya, Shanty, Raghu, & Mohanan, 2023). Furthermore, Schiff bases can be used as chemosensors in analytical chemistry, among other areas (Ejiah, Rofiu, Oloba-Whenu, & Fasina, 2023), corrosion inhibitors (Boulechfar et al., 2023), dyes (Rajimon, Elangovan, Amir Khairbek, & Thomas, 2023; Wu, Bhamidipati, Coles, & Rao, 2004), optical data storage systems and NLO materials (Hadigheh Rezvan & Aminivand, 2024), and phases in the synthesis of organic compounds (Babaei et al., 2024; Sule, Obiyenwa, Salawu, & Semire, 2025).

Interest in the benzothiazole moiety's biological importance has persisted. In 2015, Singh et al. synthesized a series of benzothiazole-Schiff bases, which were evaluated for possible antibacterial action (Singh, Kumar Singh, Thakur, Ray, & Singh, 2015). Previous studies have investigated the antimicrobial properties, quantitative structure-activity relationships, and potential mechanisms for the efficacy of benzothiazole Schiff base hybrids (Singh et al., 2017). Additionally, the antimicrobial inhibitory properties by examining their binding to lipopolysaccharides (LPS) and the depolarization of both the outer and cytoplasmic membranes were also investigated. The antimicrobial study of the compounds of interest against bacteria revealed that nine out of twenty of the benzothiazole-Schiff hybrids showed a certain degree of antimicrobial activity, as represented in Table 1. The inhibition of the growth of bacteria with good to excellent MIC values ranging between 1 and 100 μg/mL (Singh et al., 2017).

Table 1. MIC (μg/mL) of benzothiazole-Schiff bases against tested bacteria (Singh et al., 2017)

Cpd code	*S. aureus*	*E. coli*
S01	31.2	15.6
S02	31.2	15.6
S05	31.2	62.5
S08	15.6	3.91
S13	7.81	15.6
S15	3.91	7.81
S17	31.2	62.5
S19	7.81	15.6
S20	15.6	15.6
Ciprofloxacin	≥ 6.25	≥ 6.25

A deeper comprehension of molecular characteristics and interaction mechanisms at the atomic level is made possible by computational tools, which are a potent complement to experimental approaches that offer priceless insights into the antibacterial efficacy of new drugs. Calculations using Density Functional Theory (DFT) are essential for forecasting and clarifying molecules' electronic structures and global reactivity indices, which are essential for comprehending

their stability and chemical behavior (Semire, Mutiu, & Oyebamiji, 2017). Additionally, possible drug candidates' binding affinities and modes of interaction with certain biological targets, including bacterial enzymes, can be accurately predicted using a molecular docking simulation, which helps to guide rational drug design (Meng, Zhang, Mezei, & Cui, 2011). The pharmacokinetic and toxicological profiles of compounds are predicted by Absorption, Distribution, Metabolism, Excretion, and Toxicity (ADMET) studies, which are also crucial *in silico* evaluations that help eliminate inappropriate drug candidates early in the discovery pipeline and cut down on the time and expense of drug development (El-Shamy et al., 2022).

In this study, *in silico* analysis of benzothiazole Schiff base hybrids (S08, S13, S15, and S19) taken from Singh et al., (2017) As shown in Table 1, were carried out by comparing the empirically derived Minimum Inhibitory Concentrations (MICs) against a variety of microbial strains (*S. aureus* and *E. coli*) with their theoretically derived electronic characteristics utilizing DFT, forecasted binding affinities through molecular docking methodologies, and ADMET profiles. These synergistic computational and experimental methodologies aspire to furnish a profound understanding of their structure-activity relationships, elucidate prospective molecular mechanisms, and ultimately inform the rational design and advancement of more efficacious antimicrobial agents. The 2-D and optimized 3-D structures of the benzothiazole Schiff base hybrids are illustrated in Figure 1 and Supplementary Figure S1.

Cpd code	2-D Structure	Optimized 3-D Structure
S08	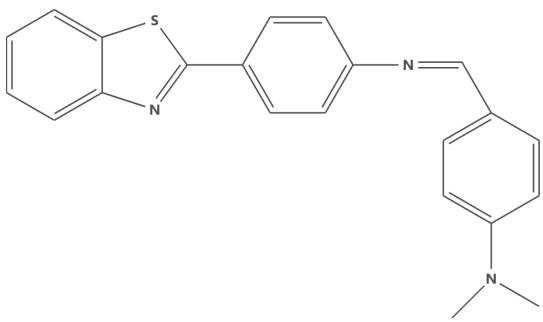	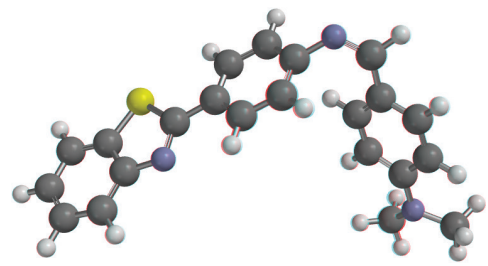
	4-(((4-(benzo[d]thiazol-2-yl)phenyl)imino)methyl)-N, N-dimethylaniline	
S13	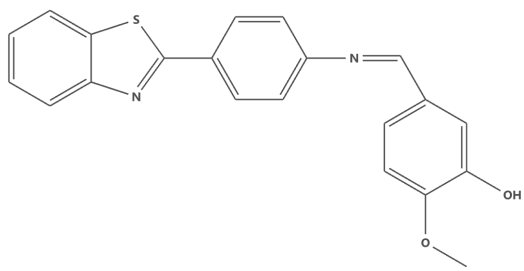	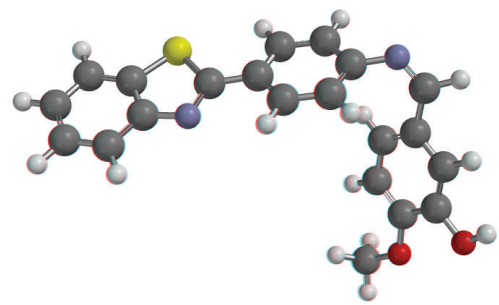
	5-(((4-(benzo[d]thiazol-2-yl)phenyl)imino)methyl)-2-methoxyphenol	

S15

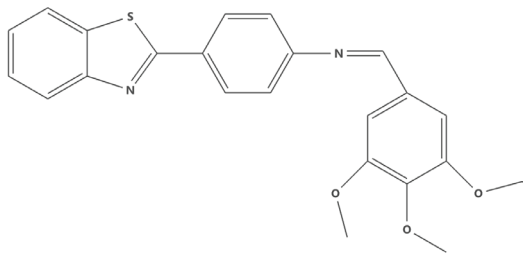

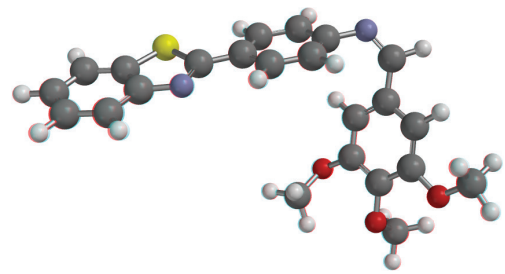

4-(benzo[d]thiazol-2-yl)-N-(3,4,5-trimethoxybenzylidene)aniline

S19

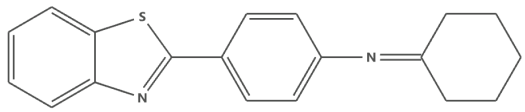

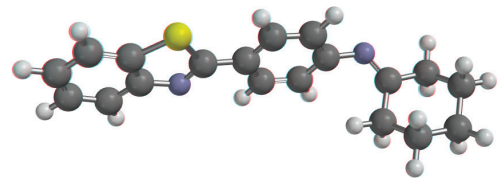

4-(benzo[d]thiazol-2-yl)-N-cyclohexylideneaniline

Figure 1. Chemical structures of the selected benzothiazole-Schiff base hybrids (S08, S13, S15, S19) investigated in this study. The complete set of 2D and optimized 3D structures for all synthesized hybrids (S01-S20) is provided in **Supplementary Figure S1**.

MATERIALS AND METHODS

DFT calculations

Using Spartan v2014 software, selected benzothiazole Schiff base hybrids and standard drug (ciprofloxacin) were optimized using the DFT approach, which is represented in the Becke-3 Parameter-Lee-Yang-Parr (B3LYP) model and the 6-31G** basis set (El-Shamy et al., 2022). The compounds S08, S13, S15, and S19 show excellent to excellent results with the MIC of these agents from 3.91 to 15.6 μg/mL (Singh et al., 2017), indicating they have strong antimicrobial potential. Ciprofloxacin was chosen as the reference because it is well-known for its effectiveness and because it specifically stops bacteria by targeting DNA gyrase, which is the main focus of our docking studies (Hooper, 2001; Singh et al., 2017).

Preliminary conformational searches of all compounds utilizing the Monte Carlo search technique and the MMFF method served as the foundation for the DFT calculations (Paul, Dilipkumar Singh, Bedamani Singh, & Sarkar, 2015). The default parameters utilized in the Spartan 14 software served as the convergence criteria for the energy calculations and geometry optimizations employed in the computations (Semire et al., 2017). The molecular parameters such as the frontier orbital energies, LOMO energy (E_{LUMO}), HOMO energy (E_{HOMO}) and energy gap ($\Delta E = (E_{LUMO} - E_{HOMO})$) and reactivity indicators, like chemical hardness ($\eta = (\Delta E)/2$), chemical potential ($\mu = (E_{LUMO} + E_{HOMO})/2$), chemical softness ($S = 1/2\eta$), overall electrophilicity ($\omega = \mu^2/2\eta$), and electronegativity ($\chi = -\mu$) are evaluated to determine the stable characteristics of these in a biological environment (Ouhazza et al., 2025; Semire et al., 2017).

Molecular docking simulations

The use of PyRx version 0.8 facilitated the assessment of the binding affinity and interactions between the benzothiazole Schiff base hybrids (S08, S13, S15, and S19) and the standard antibiotic ciprofloxacin, targeting two bacterial proteins (**4URO** and **6F86**). The three-dimensional structures of *Staphylococcus aureus* (Crystal Structure of Staphylococcus GyraseB 24kDa in complex with Novobiocin, PDB ID: **4URO**),

and *Escherichia coli* (Crystal Structure of *E. coli* GyraseB 24kDa in complex with 4-(4-bromo-1H-pyrazol-1-yl)-6-[(ethylcarbamoyl)amino]-N-(pyridin-3-yl)pyridine-3-carboxamide, PDB ID: **6F86**), with respective resolutions of 2.40 Å, and 1.90 Å were procured from the RCSB Protein Data Bank website (http://www.rcsb.org/pdb). The missing hydrogen atoms, secondary structures assigned, and Ramachandran plots were carried out to repair the proteins using the online protein repair server (Nnyigide, Nnyigide, Lee, & Hyun, 2022), as shown in Figure 2 and Supplementary Figure S2. The Autodock tool version 1.5.7 was utilized to prepare the protein receptors, removing water molecules, incorporating polar hydrogen atoms, and allocating Gasteiger charges to the receptor atoms. Subsequently, the rigid protein PDBQT files were archived (El-Shamy et al., 2022).

The ligand structures were prepared using the Molecular Operating Environment (MOE) version 2015 software. The protonation state was determined based on a physiological pH of 7.4, and energy minimization was performed using the MMFF94x force field to achieve a stable three-dimensional conformation. The final ligand structures were then exported for the docking process.

In PyRx, the grid box established by the Vina wizard grid was delineated manually to encompass the complete ligand binding site, and the correct active site was confirmed by redocking the co-ligand. The total quantity of generated binding conformations was constrained to 10 solutions. The binding conformations of each ligand in conjunction with the receptor were scrutinized utilizing Discovery Studio software 2019 (Ouhazza et al., 2025; Trott & Olson, 2010).

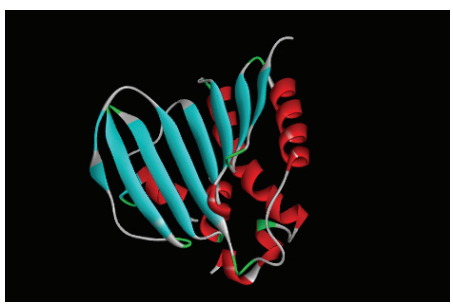

4URO

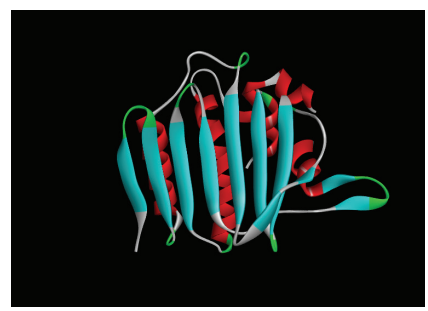

6F86

Figure 2: Three-dimensional structures of the repaired bacterial enzyme targets used for molecular docking: *S. aureus* **Gyrase B (4URO)** and *E. coli* **Gyrase B (6F86)**. The complete set of validation data, including Ramachandran plots and secondary structure assignments, is available in **Supplementary Figure S2**.

Drug-likeness and ADMET evaluation

Drug-likeness is a way to match a drug's physicochemical properties with the biological properties that the human body requires (El-Shamy et al., 2022). Lipinski's five rules state that a drug's likeness is a criterion for evaluating an active medication as a potential therapeutic candidate (Benet, Hosey, Ursu, & Oprea, 2016; Erol, Celik, & Kuyucuklu, 2021). Oral drugs should not break more than one of Lipinski's rules: the molecular weight (MW) should not be greater than 500 g/mol, the octanol/water partition coefficient (log P) value should not be greater than 5, and the chemical structures should not contain more than ten hydrogen bond acceptors (HBA) and five hydrogen bond donors (HBD) (Daina, Michielin, & Zoete, 2017).

The drug-likeness properties of the compounds were analyzed using the SwissADME tool (Listyarini, 2021; Macabeo et al., 2020). The SwissADME tool and pkCSM web server were used to estimate the drugs' ADMET profile, toxicity evaluation, and cardiotoxicity prediction (Lipinski, Lombardo, Dominy, & Feeney, 1997; Macabeo et al., 2020).

RESULTS AND DISCUSSION

DFT calculations

In DFT calculations, examining electronic energies has become crucial for understanding molecular stability and reactivity (El-Shamy et al., 2022). Koopmans' theorem provides a theoretical framework to relate the chemical behavior of molecules to their electronic properties (Tsuneda, Song, Suzuki, & Hirao, 2010).

Quantum chemical descriptors based on Koopmans' theorem can analyze a molecule's reactivity, including parameters like hardness (η), softness (S), chemical potential (μ), electronegativity (χ), and electrophilicity (ω), as shown in Table 2. Electron transfer between chemical entities occurs via molecular frontier orbitals, analyzed at the B3LYP/6–31** theoretical level (Ejalonibu et al., 2020). The Lowest Unoccupied Molecular Orbital (LUMO) and the Highest Occupied Molecular Orbital (HOMO), respectively, indicate a molecule's ability to accept and donate electrons, as displayed in Table 2 (Akbari et al., 2024).

The energy gap (ΔE) is a key quantum property of the benzothiazole-Schiff base hybrids, providing important insights into these molecules (Elangovan et al., 2024). Molecules with a smaller ΔE require less excitation energy, classifying them as chemically soft. The ΔE was calculated for each molecule; a large ΔE suggests lower chemical reactivity because it is energetically unfavorable to add an electron to the high LUMO or remove one from the low HOMO (Manolopoulos, May, & Down, 1991; Ruiz-Morales, 2002). The ΔE values of the Schiff base compounds S08 (4.08 eV), S13 (4.07 eV), S15 (4.05 eV), and S19 (4.11 eV) are markedly lower than that of ciprofloxacin (4.36 eV). This observation implies that S13, S15, and S19 may exhibit a greater propensity to participate in charge transfer interactions with biological targets in comparison to the reference drug, which correlates with their remarkable Minimum Inhibitory Concentrations (MICs) ranging from 3.91 to 15.6 μg/mL (Singh et al., 2017).

Chemically soft molecules are defined by their enhanced bioactivity (Miar, Shiroudi, Pourshamsian, Oliaey, & Hatamjafari, 2021). The biological efficacy is also dependent on the electrophilicity descriptors. Biological reactivity escalates with an increase in the electrophilicity index and chemical softness (Maria Julie et al., 2021). Electrophilicity (ω) functions as a metric of the electrophilic nature of a chemical species; it quantifies the propensity of a molecule to accept an electron, with higher values indicating pronounced electrophilicity within a molecule. The following categorization ranks organic molecules according to their electrophilicity; weak electrophiles are designated as having values below 0.8 eV, moderate electrophiles fall within the range of 0.8 to 1.5 eV, and strong electrophiles exceed 1.5 eV (Edim et al., 2021). In this investigation, all the Schiff base compounds exhibited greater electrophilicity than ciprofloxacin (ω = 2.667 eV). S15 emerged as the strongest electrophile (ω = 3.156 eV), succeeded by S19 (ω = 2.972 eV), followed by S13 (ω = 2.933 eV), and finally S08 (ω = 2.669 eV).

Chemical hardness (η) and softness (S) serve as critical parameters for elucidating stability (Domingo, Ríos-Gutiérrez, & Pérez, 2016). Ciprofloxacin, characterized by the highest hardness and the lowest softness, emerges as the most stable and least reactive entity within the studied molecular set. Conversely, the remaining compounds exhibit comparatively greater chemical softness. Compound S15 manifests the highest softness (S = 0.247 eV-1) among the hybrids, which correlates with its pronounced electrophilicity, thereby aligning with its impressive MIC values, which range from 3.91 to 7.81 μg/mL against various bacterial targets (Singh et al., 2017). Molecules exhibiting softness are generally more polarizable and are associated with enhanced bioactivity due to their capacity to readily deform their electron clouds for effective interaction with biological receptors (Miar et al., 2021).

The chemical potential (μ) serves as an indicator of the propensity for a chemical reaction; a heightened value (less negative) signifies an augmented likelihood of electron donation (acting as an electron donor), whereas a diminished value (more negative) indicates a stronger inclination towards electron acceptance (functioning as an electron acceptor) (Domingo et al., 2016). Electronegativity (χ) quantitatively assesses a molecule's capacity to attract electrons (Karton & Spackman, 2021). Density functional theory calculations elucidate significant interrelations between electronic structure and biological activity. The values for electronegativity (χ) and chemical potential (μ) remain invariant across the compounds (χ = -μ) (Hosny, Samir, & Abdel-Rhman, 2024), with S15 demonstrating the most pronounced electron-withdrawing capacity (χ = -3.575 eV, μ = 3.575 eV). The elevated electronegativity of S15 amplifies its biological activity, resulting in broad-spectrum efficacy (MICs = 3.91 to 7.81 μg/mL) (Domingo et al., 2016). S19 presents intermediate parameters (χ = -3.495 eV, μ = 3.495 eV), leading to favorable experimental MIC results (7.81 to 15.6 μg/mL). The well-balanced electronic characteristics of S08 (χ = -3.300 eV, μ = 3.300 eV) correspond with its outstanding experimental MIC values of 3.91 to 7.81 μg/mL against bacterial strains (Singh et al., 2017). These findings underscore the significance of electronegativity and chemical potential as robust predictors of antimicrobial efficacy within benzothiazole-Schiff base hybrids, positing that optimal electron-withdrawing properties enhance target-specific interactions while ensuring sufficient bioavailability (Domingo et al., 2016).

The dipole moment values elucidate a molecule's intrinsic polarity. Ciprofloxacin demonstrates a high polarity (8.2 Debye), thereby promoting solubility in aqueous environments. S19 and S15 exhibit moderate dipole moment values (3.07 and 2.86 Debye, respectively). This balanced polarity is advantageous, suggesting a favorable equilibrium in which the molecules possess adequate solubility for transport within bodily fluids, while maintaining sufficient non-polar characteristics to facilitate interaction with and penetration of the hydrophobic barriers of cellular membranes (Arnott & Planey, 2012). The HOMO and LUMO overlay S08, S13, S15, S19, and ciprofloxacin display in Figure 3.

Table 2. Global reactivity indices for the S08, S13, S15, S19 and Ciprofloxacin

Cpd Code	HOMO (eV)	LUMO (eV)	ΔE (eV)	η (eV)	μ (eV)	χ (eV)	S (eV^{-1})	ω (eV)	Dipole moment (Debye)
S08	-5.34	-1.26	4.08	2.04	-3.300	3.300	0.245	2.669	6.72
S13	-5.49	-1.42	4.07	2.035	-3.455	3.455	0.246	2.933	5.21
S15	-5.6	-1.55	4.05	2.025	-3.575	3.575	0.247	3.156	2.86
S19	-5.55	-1.44	4.11	2.055	-3.495	3.495	0.243	2.972	3.07
Ciprofloxacin	-5.59	-1.23	4.36	2.18	-3.41	3.41	0.229	2.667	8.2

Cpd code	HOMO	LUMO
S08	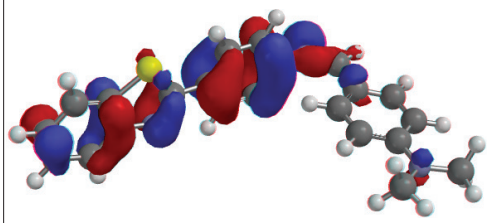	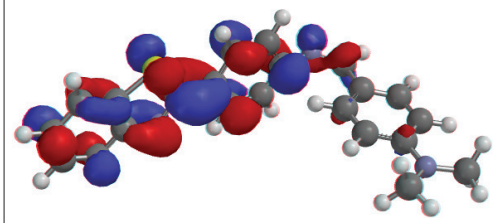
S13	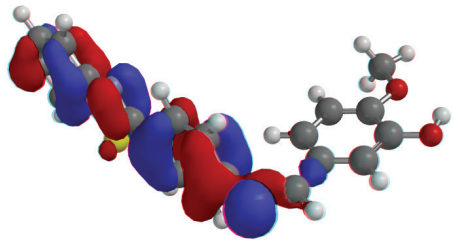	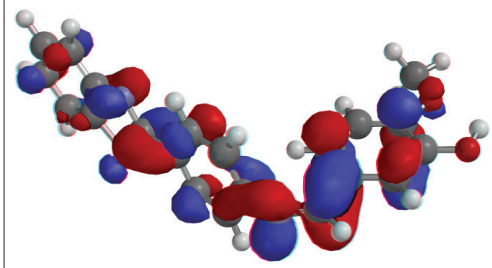
S15	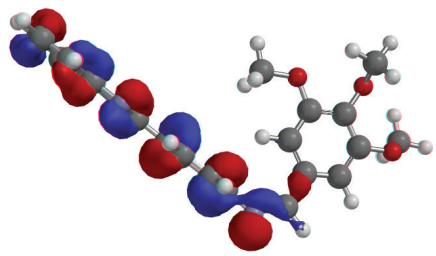	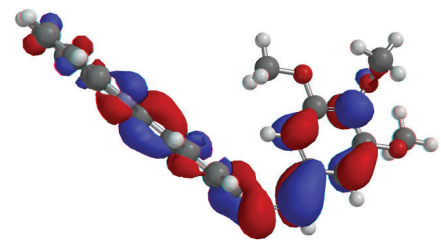
S19	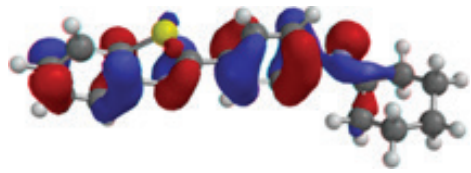	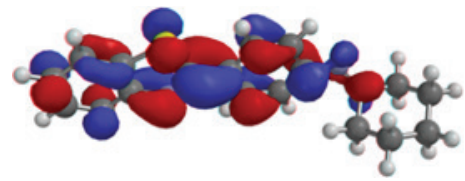
Ciprofloxacin	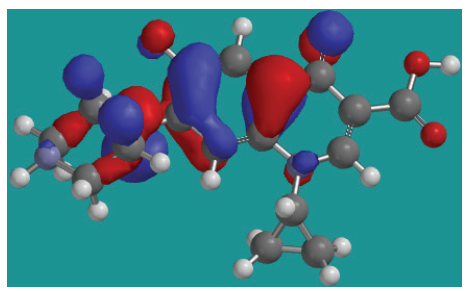	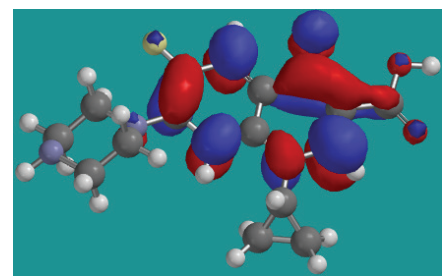

Figure 3: Frontier molecular orbitals: HOMO and LUMO of S08, S13, S15, S19, and Ciprofloxacin.

Charge distribution analysis

One of the most efficacious methodologies for determining the charge population distributions within a molecular entity in the realm of quantum chemistry is the Mulliken charge analysis (Semire et al., 2017). The distribution of electronic charges (electron density) on selected heteroatoms can provide insights into variations in the vibrational spectrum, which subsequently influences numerous additional characteristics of the system, including atomic bond lengths, dipole moments, electronic architectures, molecular polarizability, and acid-base properties (Preethi, Vijukumar, AnilaRaj, & Vidya, 2024). Furthermore, various chemical reactions, along with the physicochemical

attributes of substances, are contingent upon the electron densities. (Semire et al., 2017; Sule et al., 2025).

Various arrangements of electrons in benzothiazole-Schiff base hybrids are depicted in Table 3 through Mulliken charge analysis, which is associated with their ability to combat bacteria. Between -0.518 and the negative charge of N1, the nitrogen atom in its imine group has. This facilitates the formation of hydrogen bonds between the bacteria's targets (Domingo et al., 2016). The finding is consistent with previous research that has shown that nitrogen atoms with higher electron numbers in Schiff bases are more effective at killing bacteria because they have greater connectivity with their targets (Singh et al., 2017). S08, S13, and S15, along with their respective positive charges of 0.200 to 0.205, all have a minor positive charge in the thiazole ring (S1). The sulfur is responsible for binding the molecule to bacteria by creating weak interactions, like hydrophobic or van der Waals forces, in the region where it binds. This finding indicates this (Meng et al., 2011).

Table 3. Mulliken Charge for S08, S13, S15, S19 and Ciprofloxacin at B3LYP/6-31** basis set

Mulliken Charge								
	O1	O2	O3	N1	N2	N3	S1	F1
S08	----	----	----	-0.598	-0.456	-0.507	0.2	---
S13	0.565	-0.555	----	-0.519	-0.448	-0.519	0.202	---
S15	-0.535	-0.531	-0.526	-0.518	-0.448	----	0.204	---
S19	----	----	----	-0.518	-0.488	----	0.205	---
Ciprofloxacin	-0.511	-0.515	-0.466	-0.565	-0.536	-0.503		---

Molecular electrostatic potential (MEP)

The Molecular Electrostatic Potential (MEP) functions as an advanced quantum computational mechanism that delineates the charge distribution within a molecular entity, thereby offering valuable insights into its chemical reactivity (Aljameel, 2022; Arulaabaranam, Muthu, Mani, & Ben Geoffrey, 2021). The zones characterized as nucleophilic, electrophilic, and neutral are represented through distinct blue, red, and green color gradients, respectively (Pal et al., 2021). The MEP surfaces are illustrated in Figure 4. The spatial distribution of charge across the molecular surface imparts comprehensive information regarding its responsiveness, specifically concerning how it reacts and interacts with incoming molecular species (Maria Julie et al., 2021).

In this analytical framework, elevated negative values of MEP indicate the attraction of hydrogen ions or lighter cations within the red regions, where electron density is more concentrated at the molecular interface. Conversely, positive values of MEP denote a repulsive interaction towards protons or lighter cations in the blue regions, characterized by a diminished concentration of electron density (Miar et al., 2021). In the analyzed Schiff base compounds (S08, S13, S15, and S19), the negatively charged zones are predominantly located on the nitrogen atoms of the imine functionalities, as well as on the oxygen atoms and thiazolyl nitrogen atoms.

Consequently, these specific atoms and sites exhibit a heightened propensity to undergo electrophilic attack and engage in bond formation, such as hydrogen bonding interactions with the active sites of target proteins. Simultaneously, the positively charged zones of the compound are distributed along the hydrogen atoms of the benzothiazolyl moiety and the carbon atoms within the same group. The atoms or functional groups situated in the blue regions are susceptible to nucleophilic attack and are capable of participating in hydrophobic interactions (Abedin, Pal, Chanmiya Sheikh, & Alam, 2024).

In contrast, the chemical structure of ciprofloxacin causes its charge distribution to be dissimilar on an MEP surface. In the carboxylic acid and ketone group,

the carbonyl oxygens have the most negative potential, while the positive potential is concentrated over the protonated nitrogen in the piperazine ring and the C-H bond (Arulaabaranam et al., 2021). Its unique binding mode is accounted for by its distinct MEP map, which relies on the ionic and hydrogen bond interactions of its charged functional group (Meng et al., 2011).

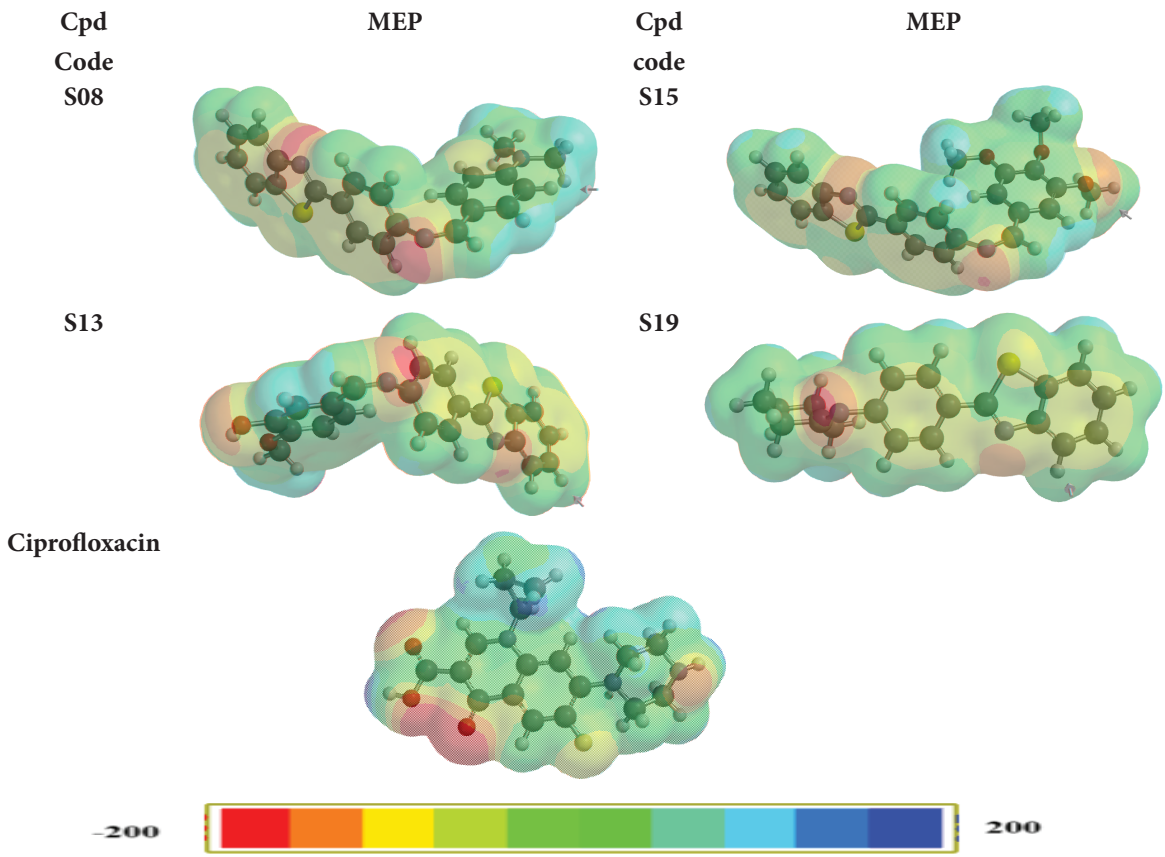

Figure 4. The Molecular Electrostatic Potential surface for S08, S13, S15, S19, and Ciprofloxacin at B3LYP/6-31** basis set

Validation of molecular docking protocol

The reliability of the molecular methodology was validated by redocking of the native co-crystallized ligands into their respective binding sites. For *S. aureus* Gyrase B (4URO), the ligand **novobicin** was extracted and subsequently redocked, yielding a root mean square deviation (RMSD) of 1.03 Å between the docked conformation and the original crystallographic pose. Similarly, for *E. coli* Gyrase B (6F86), the native ligand **4-(4-bromo-1H-pyrazol-1-yl)-6-[(ethylcarbamoyl)amino]-N-(pyridin-3-yl)pyridine-3-carboxamide** was redocked, resulting in an RMSD of 2.04 Å.

An RMSD value below 2.5 Å is considered to be a reliable indicator for a successful reproduction of the experimental binding mode (Castro-Alvarez, Costa, & Vilarrasa, 2017; Trott & Olson, 2010). The obtained values confirmed that the docking protocol employed in this investigation is both valid and proficient in accurately replicating the observed binding mode for these targets (Figure 5.).

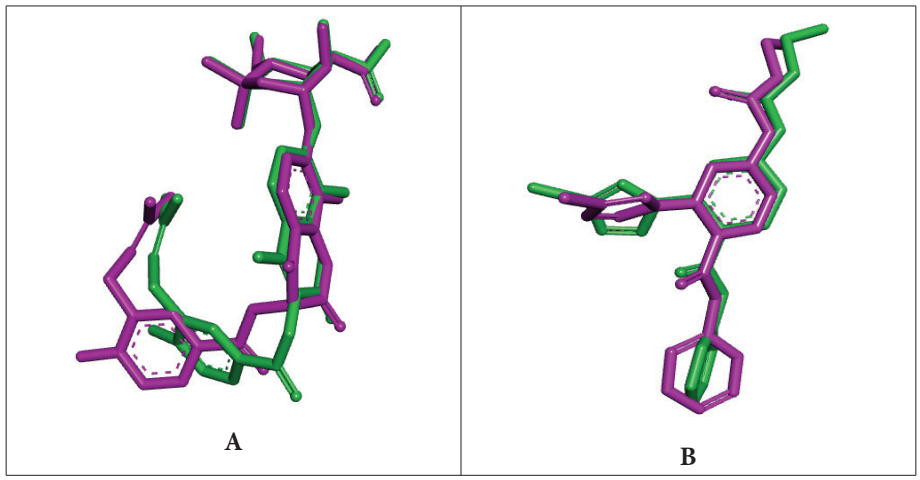

Figure 5. Validation of molecular docking protocol by superposition of crystallographic and re-docked ligand poses. **(A)** Novobiocin in the active site of *S. aureus* Gyrase B (4URO). **(B)** 4-(4-bromopyrazol-1-yl)-6-[(ethylcarbamoyl)amino]-N-(pyridin-3-yl)pyridine-3-carboxamide in the active site of *E. coli* Gyrase B (6F86). The crystallographic (native) pose is shown in green, and the re-docked pose is shown in purple.

Molecular docking

The benzothiazole Schiff base hybrids (S08, S13, S15, and S19), along with the reference antibiotic ciprofloxacin, were tested using docking simulations in the active sites of proteins from three bacteria: *S. aureus* (4URO), and *E. coli* (6F86). The results of the binding energy for these compounds are shown in Table 4. The binding energies vary from moderate to strong across the two targets (Meng et al., 2011).

S19 showed the best binding affinity against 6F86 with a value of -7.9 Kcal/mol, which is better than ciprofloxacin. This explains why S19 had good experimental MIC values (7.81 to 15.6 µg/mL) as listed in Table 1 (Singh et al., 2017). This strong binding isn't a coincidence. It's supported by S19 having a good balance of ΔE (4.11eV) and electrophilicity (ω=2.972 eV), which means it can react well with the target but still stay stable, making it a good inhibitor (Domingo et al., 2016).

S15, which had the best MIC values (3.91 to 7.81 µg/mL), also showed a strong binding energy of -6.9 Kcal/mol against 6F86. This strong activity is because of its high electrophilicity (ω = 3.156 eV) and low softness (S = 0.247 eV^{-1}), which means it can accept electrons and adjust its electron cloud to fit tightly in the enzyme's binding pocket (Miar et al., 2021). S13 had the strongest binding energy against 4URO and matched its good MIC value of 7.81 µg/mL against S. aureus (Trott & Olson, 2010).

Table 4. Binding energy of the docked benzothiazole Schiff base hybrids (S08, S13, S15, and S19) and standard drug (Ciprofloxacin) with different bacterial receptors

Cpd Code	*S.aureus* (4URO) (Kcal/mol)	*E.coli* (6F86) (Kcal/mol)
S08	-5.7	-6.7
S13	-6.9	-6.7
S15	-5.5	-6.9
S19	-5.9	-7.9
Ciprofloxacin	-5.7	-7.0

Molecular interactions

Figures 6 and 7 present the two-dimensional and three-dimensional interaction diagrams pertinent to compounds S08, S13, S15, and S19 alongside the standard antibiotic ciprofloxacin, in association with *S. aureus* (4URO), and *E. coli* (6F86), respectively.

The analyses of interactions with *S. aureus* Gyrase B (4URO), presented in Figure 6, elucidate the varying binding modalities attributable to the specificities

of this enzyme's active site. Structural studies have clearly shown that the active site of *S.aureus* Gyrase B (4URO) has a typical ATP-binding pocket, with key residues such as ASP57 and GLU58 involved in attaching natural inhibitors like novobiocin (Lu et al., 2014). Encouragingly, our docking results match this pattern exactly. The interactions associated with S19 encompass a combination of attractive charge interaction with GLU 58, a conventional hydrogen bond with ASP 57, and stabilization via hydrophobic interactions (Pi-Cation, Pi-Anion, and Pi-Alkyl) with residues ASP 67, ARG 84, GLU 58, ALA 61, and PRO 87 (Pinzi & Rastelli, 2019).

Compound S08 exhibits a conventional hydrogen bond interaction with ASP 57 and a salt bridge formation with GLU 58. It is further stabilized by a series of hydrophobic interactions, including Pi-Cation, Pi-Anion, and Pi-Alkyl interactions with residues such as ALA 61, GLU 58, PRO 87, and ARG 84.

The way S13 binds is because of hydrogen bonds with ASP 57, ARG 84, and GLU 58, a carbon-hydrogen bond with GLY 85, and Pi-Alkyl bonds with PRO 87, ALA 61, and LEU 60. These multiple hydrogen bonds and hydrophobic contacts help S13 stick strongly to *S. aureus*. Hydrogen bonds help guide the binding, while the hydrophobic interactions make the overall binding stronger (Fischer, Smieško, Sellner, & Lill, 2021; Meng et al., 2011).

Compound S15 demonstrates an attractive charge interaction with GLU 58; however, it is predominantly reliant on hydrophobic interactions (Pi-Anion, Pi-Sigma, and Pi-Alkyl) with residues including ILE 102, GLU 58, and ALA 61.

The notable abundance of hydrogen bonding interactions endows the compounds with considerable pharmacological significance, as the presence of hydrogen bonds markedly affects the pharmacological efficacy of ligands (Meng et al., 2011). This underlines the rationale for the compounds exhibiting excellent to good activity against *S. aureus*, as evidenced by their experimental MICs, which span from 3.91 to 15.6 µg/mL (Singh et al., 2017).

Conventional hydrogen bond interactions with ARG 58 and GLN 91 are responsible for the interaction between ciprofloxacin and the *S.aureus* protein. It also forms hydrophobic interactions like Pi-cation and alkyl interactions with residues like PRO 87, ILE 86, and ARG 84. This diverse array of interactions highlights the drug's effective anchoring within the active site of the *S.aureus* protein (Trott & Olson, 2010).

Cpd Code	2-D	3-D
S08	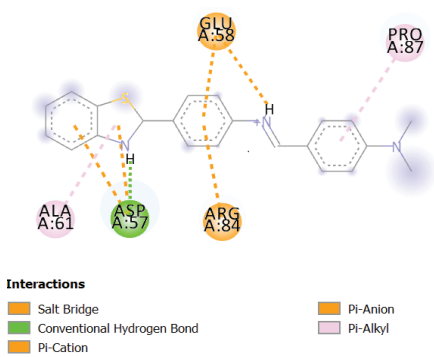	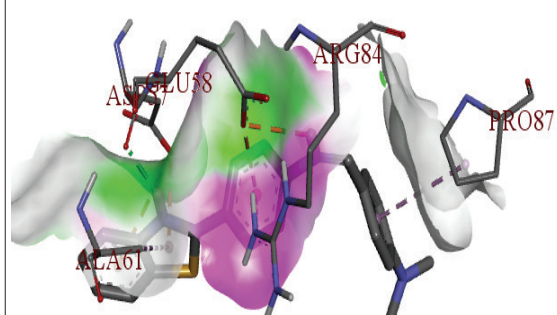

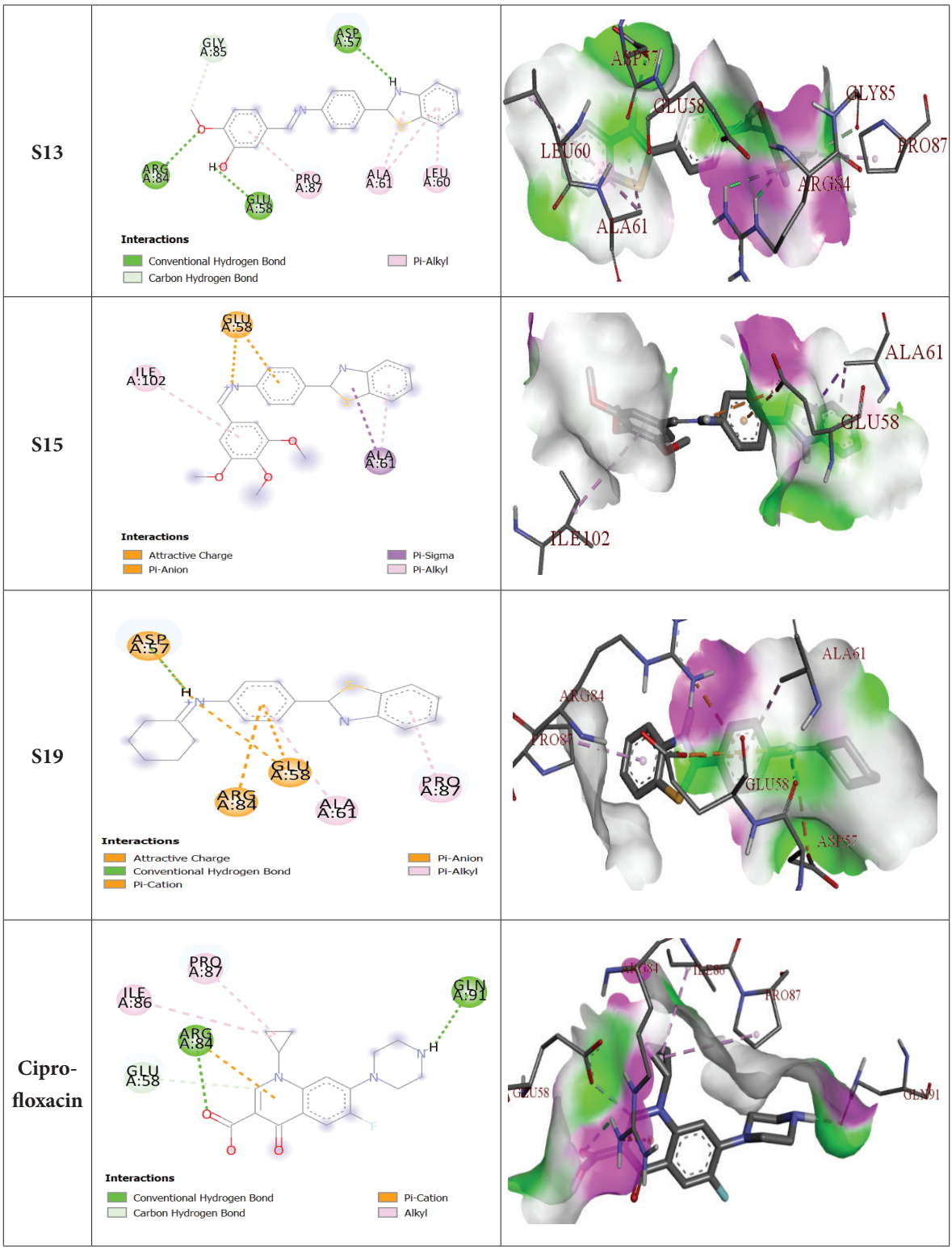

Figure 6. Two and three-dimensional interactions of S08, S13, S15, S19, and Ciprofloxacin against *S. aureus* (**4URO**)

In the interaction diagrams shown in Figure 7 for Schiff base hybrids and *E. coli* Gyrase (6F86), the active site has a deep pocket that is mostly made up of hydrophobic molecules, with some polar amino acids, such as ASP73 and GLU50, acting as binding points for synthetic inhibitors (Narramore, Stevenson, Lawson, Maxwell, & Fishwick, 2019). This is exactly what we observed with our top candidate, S19. S19 forms a salt bridge with ASP 73 and a regular hydrogen bond with GLY 77. It also has several hydrophobic interactions with ARG 76, GLU 50, VAL 43, and VAL 167, which help keep the molecule in place (Fischer et al., 2021).

S15 makes a hydrogen bond with ASP 49, has an electrostatic attraction with GLU 50, and forms a carbon-hydrogen bond with ASP 73. It also benefits from hydrophobic interactions with GLU 50, LEU 52, ILE 78, and ALA 53, giving it a complete set of interactions (Meng et al., 2011; Pinzi & Rastelli, 2019).

S13 also forms a hydrogen bond with ASP 49, has an electrostatic attraction with GLU 50, and is supported by hydrophobic interactions that improve its binding (Arnott & Planey, 2012).

S08 mainly relies on hydrophobic interactions for its binding. For the reference drug ciprofloxacin, the diagram shows its typical binding pattern, including a hydrogen bond with ASN 46 and a halogen (fluorine) bond with GLU 50 and GLY 77. It also has additional hydrophobic interactions with ILE 78 and GLU 50. This combination shows how well-documented its mechanism of Gyrase inhibition is (Trott & Olson, 2010; Wilcken et al., 2013). The detailed interaction diagrams for all other compounds (S08, S13, S15) are provided in Supplementary Figure S3.

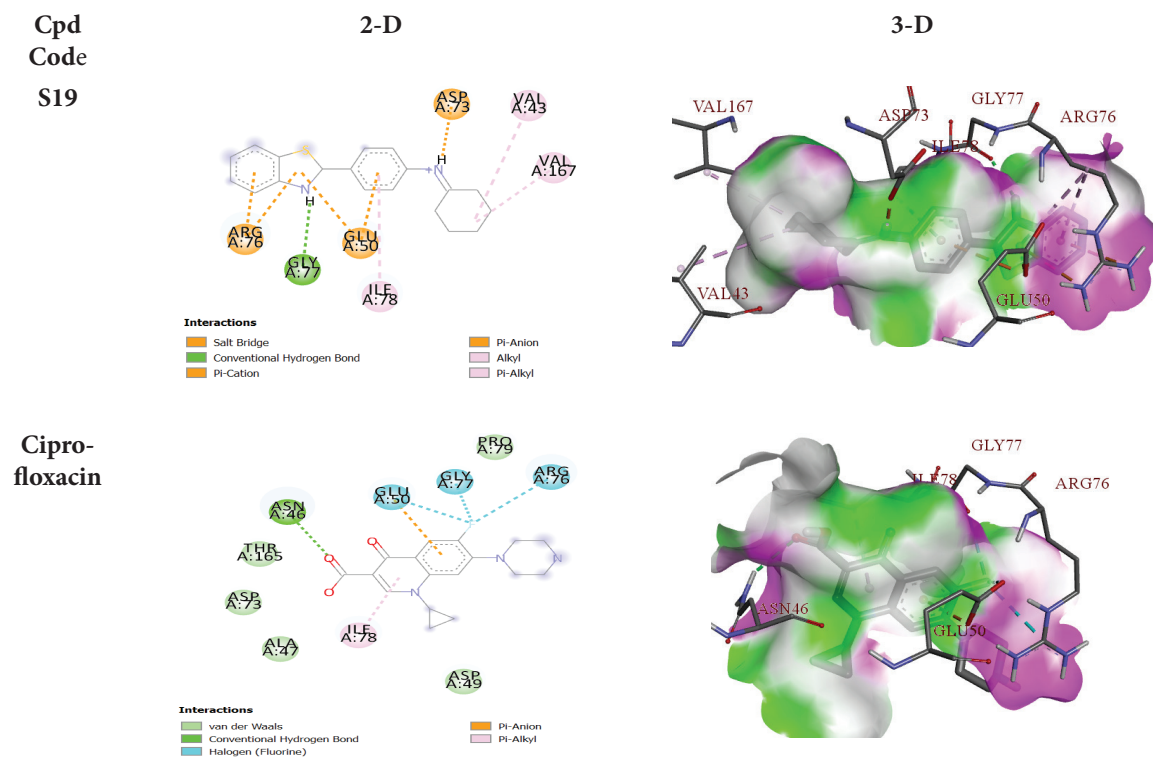

Figure 7. Molecular interactions of the lead compound S19 and the reference drug Ciprofloxacin with the active site *of E. coli* (**6F86**). The detailed interaction diagrams for all other compounds (S08, S13, S15) are provided in Supplementary Figure S3.

Drug-likeness and prediction of ADMET properties

Lipinski rule of five

Any molecular entity must exhibit distinct physical and chemical characteristics to qualify as an orally bioactive pharmaceutical agent (Ramos et al., 2020). To identify the most suitable compounds with drug-like properties, Lipinski's Rule of Five was applied. This principle posits that for a candidate molecule to be deemed appropriate for oral administration, it must demonstrate an Octanol-Water Partition Coefficient (Log P) ≤ 5, a hydrogen bond acceptor (HBA) count of ≤ 10, a molecular weight (MW) ≤ 500 g/mol, and a hydrogen bond donor (HBD) count of ≤ 5 (Lipinski et al., 1997). The criteria of Lipinski's Rule are satisfied if the compound incurs no more than one violation (Pauwels, 2004). Thus, S08, S13, S15, S19, and the standard drug (ciprofloxacin) have all adhered to Lipinski's Rule. The predicted molecular properties of the benzothiazole Schiff base hybrids satisfying Lipinski's Rule of Five are shown in Table 5.

Table 5. Predicted molecular properties of compounds satisfying Lipinski's Rule of Five

Compounds	MW(g/mol)	HBA	HBD	LogP	Lipinski Violation
S08	357.47	2	0	5.78	1
S13	360.43	4	1	5.43	1
S15	404.48	5	0	5.74	1
S19	306.42	2	0	6.00	1
Ciprofloxacin	331.34	5	2	1.18	1

ADMET properties prediction

The ADMET properties of the benzothiazole Schiff base hybrids and the standard drug that follows Lipinski's rule are listed in Table 6. S19 and ciprofloxacin are non-mutagenic, according to the Ames toxicity test, and all compounds have a high gastrointestinal absorption rate. P-glycoprotein (P-gp) is a membrane transport protein that exports toxins and pharmaceuticals outside the cell (Finch & Pillans, 2014). S19 and ciprofloxacin are found to be P-gp substrates. Moreover, the brain is protected from pathogens and toxins by the Blood-Brain Barrier (BBB), which allows selective permeability from the bloodstream to the brain (Amin, 2013; Weiss, Miller, Cazaubon, & Couraud, 2009). The BBB permeability prediction was conducted to assess the compounds' permeability; all the compounds, including the standard drug (ciprofloxacin), do not have effective Blood-Brain permeability.

Around 70-80% of pharmaceuticals in clinical settings undergo metabolic conversion via cytochrome P450 enzymes CYP3A4 and CYP2D6, which are the most relevant drug-metabolizing enzymes (Taylor et al., 2020). None of the compounds was a CYP2D6 inhibitor. S08, S13, S15, and S19 inhibited CYP3A4, indicating caution due to potential drug-drug interactions with substrates such as immunosuppressants, calcium channel blockers, and statins (Taylor et al., 2020). However, potent inhibitors of CYP3A4, like verapamil and ketoconazole, do not necessarily hinder further development of these compounds as drug candidates (Lin & Lu, 1998). Moreover, the hERG-related cardiotoxicity of compounds was predicted; none of the compounds showed action against hERG I. However, other than S19, all of the compounds inhibited hERG II. Notably, S19 and ciprofloxacin inhibited neither hERG I nor II, making them safer references (Gintant, Sager, & Stockbridge, 2016).

S19 is the best candidate based on ADMET properties, with high GI absorption and a perfect safety profile (Ames-negative, no hERG I/II inhibition). S19's structural simplicity allows for tractable optimization potential, despite its CYP3A4 inhibition and P-gp substrate activity, which are tolerable liabilities.

These options align with current FDA regulations, which prioritize safety over potency when developing early-stage antibiotics (U.S. Food and Drug Administration, 2021). S08, S13, and S15 are mutagenic, as determined by the Ames toxicity test, so they cannot be considered as potential drug candidates. Thus, S19 is identified as the top candidate through ADMET profiling.

Table 6. Predicted ADMET properties of compounds

Compound	Ames toxicity	GI Absorption	hERG I inhibitor	hERG II inhibitor	P-gp substrate	BBB Permeability	CYP3A4 inhibitor	CYP2D6 inhibitor
S08	Yes	High	No	Yes	No	No	Yes	No
S13	Yes	High	No	Yes	No	No	Yes	No
S15	Yes	High	No	Yes	Yes	No	Yes	No
S19	No	High	No	No	Yes	No	Yes	No
Ciprofloxacin	No	High	No	No	Yes	No	No	No

S19, despite its promising ADMET profile, is under scrutiny for its inhibition of cytochrome P450 3A4 (CYP3A4), the most abundant drug-metabolizing enzyme in the human liver, responsible for the oxidation of various drugs (Lin & Lu, 1998; Zanger & Schwab, 2013). This inhibition is a well-documented mechanism for drug-drug interactions (DDIs), as it can decrease the metabolic clearance of co-administered drugs, potentially increasing plasma concentrations and risk of adverse effects. Common medications that are substrates of CYP3A4 include statins, calcium channel blockers, and immunosuppressants (Guengerich, 2022).

However, CYP3A4 inhibition is often encountered in early-stage candidates and does not automatically preclude further development (Lin & Lu, 1998). Many successful drugs, such as antibiotic erythromycin and antifungal ketoconazole, are known CYP3A4 inhibitors but are used clinically with appropriate prescribing guidelines and monitoring for DDIs (Zanger & Schwab, 2013). The identification of this property in S19 is valuable for directing future medicinal chemistry efforts. The lead optimization phase could focus on structural modifications to the benzothiazole-Schiff base scaffold to mitigate CYP3A4 inhibition while preserving S19's core antimicrobial activity and safety features, such as its non-mutagenicity and lack of hERG cardiotoxicity (Hughes, Rees, Kalindjian, & Philpott, 2011).

CONCLUSION

This extensive *in silico* examination investigated the potential of benzothiazole-Schiff base hybrids (S08, S13, S15, and S19) as antimicrobial agents through the integration of DFT, molecular docking studies, and ADMET profiling. The DFT analysis indicated that the hybrids exhibit reduced HOMO-LUMO energy gaps (4.05 to 4.11 eV) and elevated electrophilicity indices (2.669 to 3.156 eV) in comparison to ciprofloxacin, suggesting enhanced chemical reactivity and improved charge transfer efficiency, which correlates with their significant experimental MIC values (3.91 to 15.6 μg/mL). Molecular docking studies corroborated robust and selective binding to bacterial gyrase targets (specifically, *S. aureus* Gyrase B and *E. coli* Gyrase B), with binding energies that are either comparable to or exceed those of the reference drug. The analysis of binding configurations revealed stabilizing interactions, encompassing hydrogen bonding and hydrophobic interactions with critical active site residues.

The assessment of drug-likeness and ADMET profiling designated S19 as the leading candidate. Although all compounds demonstrated favorable binding affinities and compliance with drug-like properties, S19 exhibited an enhanced safety profile, characterized by its non-mutagenic properties and absence of hERG cardiotoxicity concerns. Its predicted inhibition of CYP3A4 represents a manageable liability that

does not hinder the prospect of further development. In conclusion, the amalgamation of potent target affinity, advantageous electronic characteristics, and a promising ADMET profile positions S19 as a compelling candidate for further exploration. These computational findings offer a solid basis for its subsequent synthesis and empirical validation in the quest for innovative antimicrobial therapies.

AUTHOR CONTRIBUTION STATEMENT

AOS: Conceptualization, Methodology, Software, Formal analysis, Investigation, Data Curation, Writing - Original Draft. OAM: Validation, Investigation, Resources, Writing - Review & Editing. BS: Supervision, Project administration, Validation, Resources, Writing - Review & Editing, Funding acquisition.

CONFLICT OF INTEREST

The authors declare that there is no conflict of interest.

REFERENCES

Abd El-Hamid, S. M., Sadeek, S. A., Mohammed, S. F., Ahmed, F. M., & El-Gedamy, M. S. (2023). N_2O_2-chelate metal complexes with Schiff base ligand: Synthesis, characterization, and contribution as a promising antiviral agent against human cytomegalovirus. *Applied Organometallic Chemistry*, *37*(2). https://doi.org/10.1002/aoc.6958

Abdel Aziz, A. A., Ramadan, R. M., Sidqi, M. E., & Sayed, M. A. (2023). Structural characterization of novel mononuclear Schiff base metal complexes, DFT calculations, molecular docking studies, free radical scavenging, DNA binding evaluation, and cytotoxic activity. *Applied Organometallic Chemistry*, *37*(2). https://doi.org/10.1002/aoc.6954

Abedin, M. M., Pal, T. K., Chanmiya Sheik, M., & Alam, M. A. (2024). Investigation on synthesized sulfonamide Schiff base with DFT approaches and in silico pharmacokinetic studies: Topological, NBO, and NLO analyses. *Heliyon*, *10*(14). https://doi.org/10.1016/j.heliyon.2024.e34499

Akbari, Z., Stagno, C., Iraci, N., Efferth, T., Omer, E. A., Piperno, A.,… Micale, N. (2024). Biological evaluation, DFT, MEP, HOMO-LUMO analysis, and ensemble docking studies of Zn(II) complexes of bidentate and tetradentate Schiff base ligands as antileukemia agents. *Journal of Molecular Structure*, *1301*, 137400. https://doi.org/10.1016/j.molstruc.2023.137400

Alasadi, Y. K., Jumaa, F. H., & Mukhlif, M. G. (2023). Preparation, Characterization, Anti-cancer and Antibacterial Evaluation of New Schiff Base and Tetrazole Derivatives. *Tikrit Journal of Pure Science*, *28*(2), 12–19. https://doi.org/10.25130/tjps.v28i2.1333

Alfonso-Herrera, L. A., Rosete-Luna, S., Hernández-Romero, D., Rivera-Villanueva, J. M., Olivares-Romero, J. L., Cruz-Navarro, J. A.,… Colorado-Peralta, R. (2022). Transition Metal Complexes with Tridentate Schiff Bases (ONO and ONN) Derived from Salicylaldehyde: An Analysis of Their Potential Anticancer Activity. *ChemMedChem*, *17*(20). https://doi.org/10.1002/cmdc.202200367

Aljameel, A. I. (2022). DFT Study of 4-Acetamido-N-(3-amino-1,2,4-triazol-1-yl) Benzene Sulfonamide and its Potential Application as a Copper Corrosion Inhibitor. *International Journal of Electrochemical Science*, *17*(5), 220524. https://doi.org/10.20964/2022.05.39

Amin, Md. L. (2013). P-glycoprotein Inhibition for Optimal Drug Delivery. *Drug Target Insights*, *7*(1). https://doi.org/10.33393/dti.2013.1349

Arnott, J. A., & Planey, S. L. (2012). The influence of lipophilicity in drug discovery and design. *Expert Opinion on Drug Discovery*, *7*(10), 863–875. https://doi.org/10.1517/17460441.2012.714363

Aroua, L. M., Alhag, S. K., Al-Shuraym, L. A., Messaoudi, S., Mahyoub, J. A., Alfaifi, M. Y., & Al-Otaibi, W. M. (2023). Synthesis and characterization of different complexes derived from Schiff base and evaluation as a potential anticancer, antimicrobial, and insecticide agent. *Saudi Journal of Biological Sciences*, *30*(3), 103598. https://doi.org/10.1016/j.sjbs.2023.103598

Arulaabaranam, K., Muthu, S., Mani, G., & Ben Geoffrey, A. S. (2021). Speculative assessment, molecular composition, PDOS, topology exploration (ELF, LOL, RDG), ligand-protein interactions, on 5-bromo-3-nitropyridine-2-carbonitrile. *Heliyon*, *7*(5), e07061. https://doi.org/10.1016/j.heliyon.2021.e07061

Awolope, R. O., Ejidike, I. P., & Clayton, H. S. (2022). Schiff base metal complexes as dual antioxidant and antimicrobial agents. *Journal of Applied Pharmaceutical Science*. https://doi.org/10.7324/JAPS.2023.91056

Aytac, S., Gundogdu, O., Bingol, Z., & Gulcin, İ. (2023). Synthesis of Schiff Bases Containing Phenol Rings and Investigation of Their Antioxidant Capacity, Anticholinesterase, Butyrylcholinesterase, and Carbonic Anhydrase Inhibition Properties. *Pharmaceutics*, *15*(3), 779. https://doi.org/10.3390/pharmaceutics15030779

Babaei, P., Rezvan, V. H., Gilani, N. S., & Mansour, S. R. (2024). Molecular docking and in vitro biological studies of a Schiff base ligand as anticancer and antibacterial agents. *Results in Chemistry*, *7*. https://doi.org/10.1016/j.rechem.2024.101517

Benet, L. Z., Hosey, C. M., Ursu, O., & Oprea, T. I. (2016). BDDCS, the Rule of 5, and drugability. *Advanced Drug Delivery Reviews*, *101*, 89–98. https://doi.org/10.1016/j.addr.2016.05.007

Boulechfar, C., Ferkous, H., Delimi, A., Berredjem, M., Kahlouche, A., Madaci, A.,…Benguerba, Y. (2023). Corrosion inhibition of Schiff base and their metal complexes with [Mn (II), Co (II) and Zn (II)]: Experimental and quantum chemical studies. *Journal of Molecular Liquids*, *378*, 121637. https://doi.org/10.1016/j.molliq.2023.121637

Castro-Alvarez, A., Costa, A., & Vilarrasa, J. (2017). The Performance of Several Docking Programs at Reproducing Protein–Macrolide-Like Crystal Structures. *Molecules*, *22*(1), 136. https://doi.org/10.3390/molecules22010136

Daina, A., Michielin, O., & Zoete, V. (2017). SwissADME: a free web tool to evaluate pharmacokinetics, drug-likeness, and medicinal chemistry friendliness of small molecules. *Scientific Reports*, *7*(1), 42717. https://doi.org/10.1038/srep42717

Domingo, L., Ríos-Gutiérrez, M., & Pérez, P. (2016). Applications of the Conceptual Density Functional Theory Indices to Organic Chemistry Reactivity. *Molecules*, *21*(6), 748. https://doi.org/10.3390/molecules21060748

Edim, M. M., Enudi, O. C., Asuquo, B. B., Louis, H., Bisong, E. A., Agwupuye, J. A.,…Bassey, F. I. (2021). Aromaticity indices, electronic structural properties, and fuzzy atomic space investigations of naphthalene and its aza-derivatives. *Heliyon*, *7*(2), e06138. https://doi.org/10.1016/j.heliyon.2021.e06138

Ejalonibu, M. A., Elrashedy, A. A., Lawal, M. M., Soliman, M. E., Sosibo, S. C., Kumalo, H. M., & Mhlongo, N. N. (2020). Dual targeting approach for Mycobacterium tuberculosis drug discovery: insights from DFT calculations and molecular dynamics simulations. *Structural Chemistry*, *31*(2), 557–571. https://doi.org/10.1007/s11224-019-01422-w

Ejiah, F. N., Rofiu, M. O., Oloba-Whenu, O. A., & Fasina, T. M. (2023). Schiff bases as analytical tools: synthesis, chemo-sensor, and computational studies of 2-aminophenol Schiff bases. *Materials Advances*, *4*(10), 2308–2321. https://doi.org/10.1039/D3MA00097D

Elangovan, N., Sowrirajan, S., Arumugam, N., Rajeswari, B., Mathew, S., Priya, C. G.,…Mahalingam, S. M. (2024). Theoretical Investigation on Solvents Effect in Molecular Structure (TD-DFT, MEP, HOMO-LUMO), Topological Analysis and Molecular Docking Studies of N-(5-((4-Ethylpiperazin-1-yl)Methyl)Pyridin-2-yl)-5-Fluoro-4-(4-Fluoro-1-Isopropyl-2-Methyl-1H-Benzo[d] Imidazol-6-yl) Pyrimidin-2-Amine. *Polycyclic Aromatic Compounds*, *44*(7), 4467–4490. https://doi.org/10.1080/10406638.2023.2254896

El-Shamy, N. T., Alkaoud, A. M., Hussein, R. K., Ibrahim, M. A., Alhamzani, A. G., & Abou-Krisha, M. M. (2022). DFT, ADMET and Molecular Docking Investigations for the Antimicrobial Activity of 6,6′-Diamino-1,1′,3,3′-Tetramethyl-5,5′-(4-chlorobenzylidene)bis[pyrimidine-2,4(1H,3H)-dione]. *Molecules*, *27*(3). https://doi.org/10.3390/molecules27030620

Erol, M., Celik, I., & Kuyucuklu, G. (2021). Synthesis, Molecular Docking, Molecular Dynamics, DFT, and Antimicrobial Activity Studies of 5-substituted-2-(p-methylphenyl)benzoxazole Derivatives. *Journal of Molecular Structure*, *1234*, 130151. https://doi.org/10.1016/j.molstruc.2021.130151

Finch, A., & Pillans, P. (2014). P-glycoprotein and its role in drug-drug interactions. *Australian Prescriber*, *37*(4), 137–139. https://doi.org/10.18773/austprescr.2014.050

Fischer, A., Smieško, M., Sellner, M., & Lill, M. A. (2021). Decision Making in Structure-Based Drug Discovery: Visual Inspection of Docking Results. *Journal of Medicinal Chemistry*, *64*(5), 2489–2500. https://doi.org/10.1021/acs.jmedchem.0c02227

Gintant, G., Sager, P. T., & Stockbridge, N. (2016). Evolution of strategies to improve preclinical cardiac safety testing. *Nature Reviews Drug Discovery*, *15*(7), 457–471. https://doi.org/10.1038/nrd.2015.34

Guengerich, F. P. (2022). Inhibition of Cytochrome P450 Enzymes by Drugs: Molecular Basis and Practical Applications. *Biomolecules & Therapeutics*, *30*(1), 1–18. https://doi.org/10.4062/biomolther.2021.102

Hadigheh Rezvan, V., & Aminivand, Y. (2024). DFT computational study of optical properties for bis-Schiff bases of 8-aminoquinoline derivatives and furan-2, 3-dicarbaldehyde. *Structural Chemistry*, *35*(5), 1577–1587. https://doi.org/10.1007/s11224-024-02296-3

Hahn, P. (2024). Role of Heterocyclic Compounds in Drug Development: An Overview. *Research & Reviews: Journal of Medicinal and Organic Chemistry JOMC*, *11*(8). https://doi.org/10.4172/J

Hooper, D. C. (2001). Mechanisms of Action of Antimicrobials: Focus on Fluoroquinolones. *Clinical Infectious Diseases*, *32*(Supplement_1), S9–S15. https://doi.org/10.1086/319370

Hosny, N. M., Samir, G., & Abdel-Rhman, M. H. (2024). N′-(Furan-2-ylmethylene)-2-hydroxybenzohydrazide, and its metal complexes: synthesis, spectroscopic investigations, DFT calculations, and cytotoxicity profiling. *BMC Chemistry*, *18*(1), 1–17. https://doi.org/10.1186/s13065-023-01098-8

Hughes, J., Rees, S., Kalindjian, S., & Philpott, K. (2011). Principles of early drug discovery. *British Journal of Pharmacology*, *162*(6), 1239–1249. https://doi.org/10.1111/j.1476-5381.2010.01127.x

In Silico Study of Pyrazolylaminoquinazoline Toxicity by Lazar, Protox, and Admet Predictor. (2018). *Journal of Applied Pharmaceutical Science*, *8*(9), 119–129. https://doi.org/10.7324/JAPS.2018.8918

Karton, A., & Spackman, P. R. (2021). Evaluation of density functional theory for a large and diverse set of organic and inorganic equilibrium structures. *Journal of Computational Chemistry*, *42*(22), 1590–1601. https://doi.org/10.1002/jcc.26698

Krishna, G. A., Dhanya, T. M., Shanty, A. A., Raghu, K. G., & Mohanan, P. V. (2023). Transition metal complexes of imidazole-derived Schiff bases: Antioxidant/anti-inflammatory/antimicrobial/enzyme inhibition and cytotoxicity properties. *Journal of Molecular Structure*, *1274*, 134384. https://doi.org/10.1016/j.molstruc.2022.134384

Lin, J. H., & Lu, A. Y. H. (1998). Inhibition and Induction of Cytochrome P450 and the Clinical Implications. *Clinical Pharmacokinetics*, *35*(5), 361–390. https://doi.org/10.2165/00003088-199835050-00003

Lipinski, C. A., Lombardo, F., Dominy, B. W., & Feeney, P. J. (1997). Experimental and computational approaches to estimate solubility and permeability in drug discovery and development settings. *Advanced Drug Delivery Reviews*, *23*(1–3), 3–25. https://doi.org/10.1016/S0169-409X(96)00423-1

Listyarini, R. V. (2021). Implementation of the Molecular Visualization Program for Chemistry Learning. *Prisma Sains : Jurnal Pengkajian Ilmu Dan Pembelajaran Matematika Dan IPA IKIP Mataram*, *9*(1), 64. https://doi.org/10.33394/j-ps.v9i1.3941

Lu, J., Patel, S., Sharma, N., Soisson, S., Kishii, R., Takei, M., … Singh, S. B. (2014). Crystal Structure of Staph Gyrase B 24kDa in complex with Novobiocin. In the *Worldwide Protein Data Bank*. https://doi.org/10.2210/pdb4uro/pdb

Macabeo, A. P. G., Pilapil, L. A. E., Garcia, K. Y. M., Quimque, M. T. J., Phukhamsakda, C., Cruz, A. J. C.,…Stadler, M. (2020). Alpha-Glucosidase- and Lipase-Inhibitory Phenalenones from a New Species of Pseudolophiostoma Originating from Thailand. *Molecules*, *25*(4), 965. https://doi.org/10.3390/molecules25040965

Manolopoulos, D. E., May, J. C., & Down, S. E. (1991). Theoretical studies of the fullerenes: C34 to C70. *Chemical Physics Letters*, *181*(2–3), 105–111. https://doi.org/10.1016/0009-2614(91)90340-F

Maria Julie, M., Prabhu, T., Elamuruguporchelvi, E., Asif, F. B., Muthu, S., & Irfan, A. (2021). RETRACTED: Structural (monomer and dimer), wavefunctional, NCI analysis in aqueous phase, electronic and excited state properties in different solvent atmospheres of 3-{(E)-[(3,4-dichlorophenyl)imino]methyl} benzene-1,2-diol. *Journal of Molecular Liquids*, *336*, 116335. https://doi.org/10.1016/j.molliq.2021.116335

Meng, X.-Y., Zhang, H.-X., Mezei, M., & Cui, M. (2011). Molecular Docking: A Powerful Approach for Structure-Based Drug Discovery. *Current Computer-Aided Drug Design*, *7*(2), 146–157. https://doi.org/10.2174/157340911795677602

Miar, M., Shiroudi, A., Pourshamsian, K., Oliaey, A. R., & Hatamjafari, F. (2021). Theoretical investigations on the HOMO–LUMO gap and global reactivity descriptor studies, natural bond orbital, and nucleus-independent chemical shifts analyses of 3-phenylbenzo[*d*]thiazole-2(3H)-imine and its *para-substituted* derivatives: Solvent and substituent effects. *Journal of Chemical Research*, *45*(1–2), 147–158. https://doi.org/10.1177/1747519820932091

Narramore, S. K., Stevenson, C. E. M., Lawson, D. M., Maxwell, A., & Fishwick, C. W. G. (2019). Crystal Structure of E. coli GyraseB 24kDa in complex with 4-(4-bromo-1H-pyrazol-1-yl)-6-[(ethylcarbamoyl)amino]-N-(pyridin-3-yl)pyridine-3-carboxamide. In the *Worldwide Protein Data Bank*. https://doi.org/10.2210/pdb6f86/pdb

Nnyigide, O. S., Nnyigide, T. O., Lee, S.-G., & Hyun, K. (2022). Protein Repair and Analysis Server: A Web Server to Repair PDB Structures, Add Missing Heavy Atoms and Hydrogen Atoms, and Assign Secondary Structures by Amide Interactions. *Journal of Chemical Information and Modeling*, *62*(17), 4232–4246. https://doi.org/10.1021/acs.jcim.2c00571

Ouhazza, H., Abdelaziz, M., Alaoui, E., Soussi, S., Idrissi, A., Habsaoui, A., & Bouzakraoui, S. (2025). Molecular Docking, ADMET, DFT Studies, and Retrosynthesis Strategy of New Benzimidazolone Derivatives as HIV-1 Reverse Transcriptase (RT) Inhibitors. *Journal of Medicinal and Chemical Sciences*, *8*, 119–135. https://doi.org/10.26655/JMCHEMSCI.2025.2.1

Pal, T. K., Mumit, M. A., Hossen, J., Paul, S., Alam, Md. A., Islam, Md. A.-A.-A.-A., & Sheik, Md. C. (2021). Computational and experimental insight into antituberculosis agent, (E)-benzyl-2-(4-hydroxy-2-methoxybenzylidene) hydrazinecarbodithioate: ADME analysis. *Heliyon*, *7*(10), e08209. https://doi.org/10.1016/j.heliyon.2021.e08209

Paul, M. Kr., Dilipkumar Singh, Y., Bedamani Singh, N., & Sarkar, U. (2015). Emissive bis-salicylaldiminato Schiff base ligands, and their zinc(II) complexes: Synthesis, photophysical properties, mesomorphism, and DFT studies. *Journal of Molecular Structure*, *1081*, 316–328. https://doi.org/10.1016/j.molstruc.2014.10.031

Pauwels, R. (2004). New non-nucleoside reverse transcriptase inhibitors (NNRTIs) are being developed for the treatment of HIV infections. *Current Opinion in Pharmacology*, *4*(5), 437–446. https://doi.org/10.1016/j.coph.2004.07.005

Pibiri, I. (2024). Recent Advances: Heterocycles in Drugs and Drug Discovery. *International Journal of Molecular Sciences*, *25*(17), 9503. https://doi.org/10.3390/ijms25179503

Pinzi, L., & Rastelli, G. (2019). Molecular Docking: Shifting Paradigms in Drug Discovery. *International Journal of Molecular Sciences*, *20*(18), 4331. https://doi.org/10.3390/ijms20184331

Pore, A., Gaikwad, G., Hegade, S., Jadhav, Y., Mane, R., & Kumbhar, R. (2023). Analyzing the Impact of the Substituent on the Quinazolinone Schiff Base and the Interaction of the Fe (III) and Cr (III) with Different Quinazolinone Schiff Bases for Antioxidant and Anti-inflammatory Activity. *Analytical Chemistry Letters*, *13*(1), 39–59. https://doi.org/10.1080/22297928.2023.2173647

Preethi, V., Vijukumar, V. G., AnilaRaj, S., & Vidya, V. G. (2024). Synthesis, characterization, DFT studies, and evaluation of the potential anti-tumor activity of nicotinic hydrazide-based Schiff base using in vitro and molecular docking techniques. *Heliyon*, *10*(9). https://doi.org/10.1016/j.heliyon.2024.e29689

Rajimon, K. J., Elangovan, N., Amir Khairbek, A., & Thomas, R. (2023). Schiff bases from chlorine-substituted anilines and salicylaldehyde: Synthesis, characterization, fluorescence, thermal features, biological studies, and electronic structure investigations. *Journal of Molecular Liquids*, *370*, 121055. https://doi.org/10.1016/j.molliq.2022.121055

Ramos, R. S., Macêdo, W. J. C., Costa, J. S., da Silva, C. H. T. de P., Rosa, J. M. C., da Cruz, J. N.,…Santos, C. B. R. (2020). Potential inhibitors of the enzyme acetylcholinesterase and juvenile hormone with insecticidal activity: study of the binding mode via docking and molecular dynamics simulations. *Journal of Biomolecular Structure and Dynamics*, *38*(16), 4687–4709. https://doi.org/10.1080/07391102.2019.1688192

Rezaei, M. T., Keypour, H., Hajari, S., Yaghoobi, F., Moazzami Farida, S. H., Saadati, M., & Gable, R. W. (2023). Theoretical and solid-state structures of three new macroacyclic Schiff base complexes and the investigation of their anticancer, antioxidant, and antibacterial properties. *RSC Advances*, *13*(14), 9418–9427. https://doi.org/10.1039/D3RA00153A

Ruiz-Morales, Y. (2002). HOMO–LUMO Gap as an Index of Molecular Size and Structure for Polycyclic Aromatic Hydrocarbons (PAHs) and Asphaltenes: A Theoretical Study. I. *The Journal of Physical Chemistry A*, *106*(46), 11283–11308. https://doi.org/10.1021/jp021152e

Semire, B., Mutiu, O., & Oyebamiji, A. K. (2017). *DFT and AB INITIO Methods on NMR, IR, and Reactivity Indices of Indol-3-Carboxylate and Indazole-3-Carboxylate Derivatives of Cannabinoids: Comparative Study*. www.SID.ir

Singh, M., Kumar Singh, S., Thakur, B., Ray, P., & Singh, S. K. (2015). Design and Synthesis of Novel Schiff Base-Benzothiazole Hybrids as Potential Epidermal Growth Factor Receptor (EGFR) Inhibitors. *Anti-Cancer Agents in Medicinal Chemistry*, *16*(6), 722–739. https://doi.org/10.2174/1871520615666151007160115

Singh, M., Sellamuthu, S., Singh, S. K., Gangwar, M., Nath, G., & Singh, S. K. (2017). Antimicrobial Potency and Molecular Mechanism of Benzothiazole Schiff Base Hybrids. *Saudi Journal of Medical and Pharmaceutical Sciences*. https://doi.org/10.36348/sjmps.2017.v03i12.017

Sule, A. O., Obiyenwa, K. G., Salawu, O. W., & Semire, B. (2025). In silico evaluation of Co(II), Mn(II), Cu(II), and Zn(II) complexes with hydrazide ligands: DFT, spectroscopic, and molecular docking studies. *International Journal of Chemical Studies*, *13*(3), 96–113. https://doi.org/10.22271/chemi.2025.v13.i3b.12545

Taylor, C., Crosby, I., Yip, V., Maguire, P., Pirmohamed, M., & Turner, R. M. (2020). A Review of the Important Role of CYP2D6 in Pharmacogenomics. *Genes*, *11*(11), 1295. https://doi.org/10.3390/genes11111295

Trott, O., & Olson, A. J. (2010). AutoDock Vina: Improving the speed and accuracy of docking with a new scoring function, efficient optimization, and multithreading. *Journal of Computational Chemistry*, *31*(2), 455–461. https://doi.org/10.1002/jcc.21334

Tsuneda, T., Song, J.-W., Suzuki, S., & Hirao, K. (2010). On Koopmans' theorem in density functional theory. *The Journal of Chemical Physics*, *133*(17). https://doi.org/10.1063/1.3491272

U.S. Food and Drug Administration. (2021). *Novel Drug Approvals for 2021. https://www.fda.gov/drugs/novel-drug-approvals-fda/novel-drug-approvals-2021*.

Weiss, N., Miller, F., Cazaubon, S., & Couraud, P.-O. (2009). The blood-brain barrier in brain homeostasis and neurological diseases. *Biochimica et Biophysica Acta (BBA) - Biomembranes*, *1788*(4), 842–857. https://doi.org/10.1016/j.bbamem.2008.10.022

Wilcken, R., Zimmermann, M. O., Lange, A., Joerger, A. C., & Boeckler, F. M. (2013). Principles and Applications of Halogen Bonding in Medicinal Chemistry and Chemical Biology. *Journal of Medicinal Chemistry*, *56*(4), 1363–1388. https://doi.org/10.1021/jm3012068

Wu, P., Bhamidipati, M., Coles, M., & Rao, D. V. G. L. N. (2004). Biological nano-ceramic materials for holographic data storage. *Chemical Physics Letters*, *400*(4–6), 506–510. https://doi.org/10.1016/j.cplett.2004.10.129

Yassen, T. M., & AL-Azzawi, A. M. (2023). Synthesis and Characterization of New Bis-Schiff Bases Linked to Various Imide Cycles. *Iraqi Journal of Science*, 1062–1070. https://doi.org/10.24996/ijs.2023.64.3.3

Zanger, U. M., & Schwab, M. (2013). Cytochrome P450 enzymes in drug metabolism: Regulation of gene expression, enzyme activities, and impact of genetic variation. *Pharmacology & Therapeutics*, *138*(1), 103–141. https://doi.org/10.1016/j.pharmthera.2012.12.007